ARTICLE OPEN

Check for updates

Frequency-insensitive spatiotemporal shaping of single photon in multiuser quantum network

Yiwen Huang[1], Zhantong Qi[1], Yilin Yang[1], Yuanhua Li[1,2], Yiwei Sun[1], Yongzhi Tang[1], Fengchao Ni[1], Lanting Li[1], Yuanlin Zheng[1,3] and Xianfeng Chen[1,3,4]✉

Exploiting the fundamental features of quantum mechanics, an entanglement-based quantum network offers a promising platform for many dramatic applications such as multi-user cryptography. Nevertheless, the implementation of a large-scale quantum network in real-world scenarios remains challenging owing to the multiple scattering events in complex environment, particularly those frequency-sensitive scatterings that disturb quantum correlation both spatially and temporally. Here, we demonstrate the frequency-insensitive spatiotemporal control of entangled photons in a fully connected network by leveraging a Fourier-transform setup and the genetic algorithm. Such an approach can effectively improve the entanglement distribution process through a multimode fiber while the quantum characteristic of the network can be maintained well after the spatiotemporal shaping. Our scheme can serve as a bridging technology to establish entanglement between remote nodes of spectrally interconnected quantum systems and has great potential applications in future real-world quantum networks.

npj Quantum Information (2023)9:83 ; https://doi.org/10.1038/s41534-023-00752-2

INTRODUCTION

Entanglement-based quantum networks offer a promising platform for many dramatic applications, such as distributed quantum computation[1], quantum sensing[2,3], and multi-user quantum communication[4–7]. When constructing a large-scale practical quantum network, the coherent transfer of quantum information with the preservation of the delicate entanglement of photons through a noisy channel become a challenging but important issue[8–11]. When coherent light passes through a scattering medium, especially those frequency-sensitive complex media like multimode fiber (MMF), the optical field dramatically changes with the frequency of the input field due to the frequency-dependent mode coupling effect and interference, behaving as various output speckle patterns[12,13]. Such media involve the complex interplay of hundreds to millions of modes, and the effects of scattering must be overcome in a manner that preserves higher-order quantum coherence between all modes of interest[14]. In temporal imaging, propagation through a dispersive media causes the constituent frequencies of a pulse to diverge in time, resulting in a temporal disturbance of the photon pulses.

In future quantum networks, MMF has the prospect of becoming a transmission channel for quantum states encoded in multiple degrees of freedom of photons, e.g., spatial mode and frequency, and will play an important role in entanglement distribution process due to its unique characteristics in various propagation modes[15]. Recently, the wavefront shaping technique based on high-resolution SLMs has made significant progress in performing quantum information tasks through a MMF, including manipulating two-photon quantum walk[12], harnessing disorder for reconfigurable optical networks[13], and unscrambling spatial entanglement[14]. Unscrambling entangled photons through a MMF has become an important technique and is essential for constructing a heterogeneous quantum network. To effectively establish entanglement between remote nodes made of quantum memories of a quantum repeater network, the telecommunication photons need to be transferred to near-infrared photons by quantum nonlinear frequency conversion[16–20]. The temporal disturbance from the MMF will directly affect the temporal overlap degree of single photons and pump pulses[21], which may significantly reduce the quantum frequency conversion efficiency[22]. On the other hand, as an important degree of freedom (DOF), the photon frequency has been leveraged to significantly improve the capacity of an communication channel in large-scale quantum networks, particularly in those specific networks with a fully-connected topological structure[5]. When the incident light comprises multi-wavelength photon pulses, the MMF responds differently for the distinct spectral components of different pulses and produces a very complex spatiotemporal speckle pattern at the output[23]. Therefore, to implement the best quality of entanglement distribution through a frequency-sensitive MMF in future quantum network, a frequency-independent spatiotemporal shaping technique is required to compensate for both the spatial and temporal distortions for each frequency component of the quantum links[24].

Here, we demonstrate a frequency-independent spatiotemporal shaping scheme to control entangled photon pulses propagating through a frequency-sensitive complex medium, i.e. a 200-meter-long MMF. In general, the propagation through a complex medium can be described by a Transmission Matrix $\hat{\boldsymbol{\Gamma}}$, which can be acquired by using phase-shifting wavefront shaping techniques. Unlike the traditional wavefront shaping scheme[23] (Fig. 1a) which directly modulates the input optical field using a SLM, the frequency-insensitive spatiotemporal shaping scheme is based on Fourier-transform apparatus, as shown in Fig. 1b. In the Fourier-transform apparatus, the input single photon pulses are first spectrally dispersed to different spatial positions by a grating.

[1]State Key Laboratory of Advanced Optical Communication Systems and Networks, School of Physics and Astronomy, Shanghai Jiao Tong University, Shanghai 200240, China. [2]Department of Physics, Shanghai Key Laboratory of Materials Protection and Advanced Materials in Electric Power, Shanghai University of Electric Power, Shanghai 200090, China. [3]Shanghai Research Center for Quantum Sciences, Shanghai 201315, China. [4]Collaborative Innovation Center of Light Manipulation and Applications, Shandong Normal University, Jinan 250358, China. ✉email: xfchen@sjtu.edu.cn

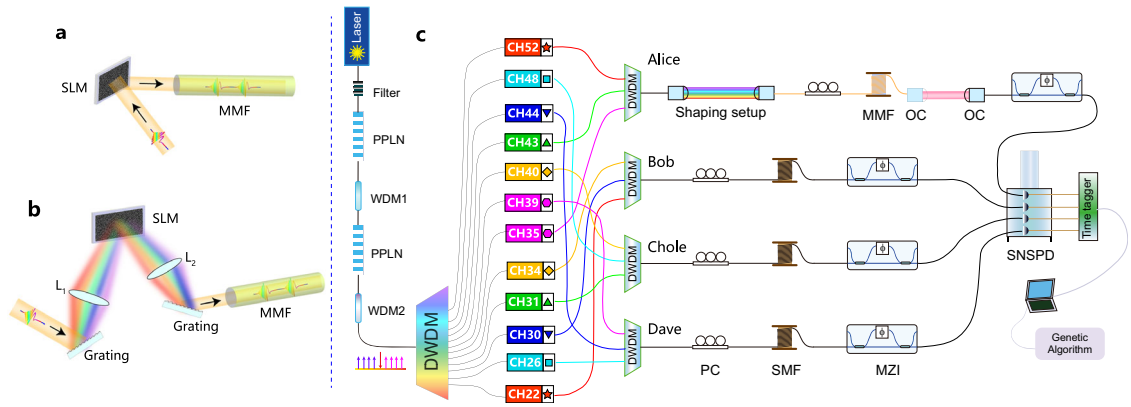

Fig. 1 Experimental setup. a Schematic of the traditional shaping setup. **b** Schematic of the Fourier transform shaping setup. **c** Experimental setup for frequency-insensitive spatiotemporal shaping of single photons. SLM spatial light modulator, L achromatic lens, WDM wavelength division multiplexing filter, DWDM dense wavelength division multiplexing filter, OC optical collimator, PC polarization controller, MMF multimode fiber, SMF single mode fiber, MZI Mach-Zehnder Interferometer, SNSPD superconducting nanowire single photon detector.

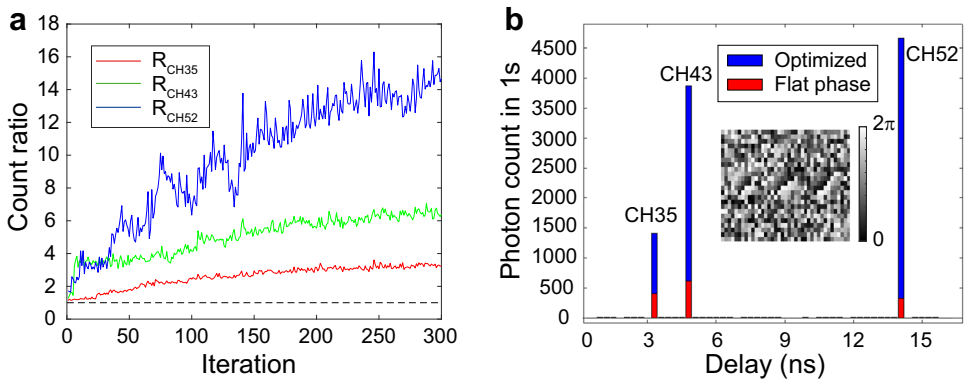

Fig. 2 Optimization processes. a Performance of the genetic algorithm for the Fourier transform shaping setup. **b** Enhancement of the entanglement distribution. The inset presents the optimal phase pattern after the shaping process.

Each angularly separated frequency component of the pulse is focused onto a specific lateral position in the focal plane of an achromatic lens, yielding an elongated focal spot where the wavelength varies from λ_{min} to λ_{max} according to the parameters of the grating and achromatic lens. A spatial light modulator (SLM) is positioned near the focal plane centered on the beam to implement the targeted masking function. After undergoing a local phase shift for pulse shaping on the SLM, the spectrum-separated single photon pulses are recombined by a second grating, yielding an output pulse of modified temporal shape and optimized wavefront controlled by the genetic algorithm. Considering the two-photon quantum state emitted in a nonlinear crystal[11,25]: $|\psi\rangle = \xi \int d\omega_i d\omega_s \Phi(\omega_i, \omega_s, \boldsymbol{q}_i, \boldsymbol{q}_s) \hat{a}^{\dagger}_{\omega_i}(\boldsymbol{q}_i, t) \hat{a}^{\dagger}_{\omega_s}(\boldsymbol{q}_s, t)|0\rangle$, where $\Phi(\omega_i, \omega_s, \boldsymbol{q}_i, \boldsymbol{q}_s)$ represents the two-photon amplitude, ξ is the coupling constant corresponding to the second-order susceptibility $\chi^{(2)}$ of the nonlinear crystal, and $\hat{a}^{\dagger}_{\omega_i}(\boldsymbol{q}_i, t)$ is the creation operator of a photon with a transverse momentum $\boldsymbol{q}_i$ and the frequency of ω_i. We suppose that only the signal photons undergo the scattering of the MMF, which brings a linear transformation Γ on the creation operator $\hat{a}^{\dagger}_{\omega_s}(\boldsymbol{q}_s, t) \rightarrow \int d\boldsymbol{\rho} \Gamma(\boldsymbol{\rho}, \omega_s) exp(i\boldsymbol{\rho} \cdot \boldsymbol{q}_s + i\phi(t))$, resulting in the output state:

$$\begin{aligned} |\psi\rangle_{out} &= (\mathbb{1} \otimes \hat{\boldsymbol{\Gamma}})|\psi\rangle \\ &= \xi \int d\omega_i d\omega_s d\boldsymbol{\rho} \Gamma(\boldsymbol{\rho}, \omega_s) \hat{a}^{\dagger}_{\omega_i}(\boldsymbol{q}_i, t) \hat{a}^{\dagger}_{\omega_s}(\boldsymbol{\rho}, t) \\ &\quad \times \Phi(\omega_i, \omega_s, \boldsymbol{q}_i, \boldsymbol{q}_s) exp(i\boldsymbol{\rho} \cdot \boldsymbol{q}_s + i\phi(\omega_s, t)), \end{aligned} \tag{1}$$

where $\Gamma(\boldsymbol{\rho}, \omega_s)$ and $\phi(\omega_s, t)$ are the amplitude and temporal transfer functions of the MMF, and $\boldsymbol{\rho}$ is the transverse spatial coordinate. The adaptive spatiotemporal shaping presents a solution to the inverse problem, i.e. the inverse matrix $\hat{\boldsymbol{\Gamma}}^{-1}$, seeking to find the unknown targeted spatial modes and temporal profiles for different frequency components of incident single photons. By adaptively compensating for the spatial and temporal disorder, we show that such a scheme can significantly improve the entanglement distribution of multi-wavelength single photon pulses through the MMF and enhance the sum frequency generation (SFG) of single photons. Our scheme can serve as a bridging technology to establish the entanglement between remote nodes of spectrally interconnected quantum systems, which is an essential prerequisite for constructing a practical long-distance quantum network.

RESULTS

Spatiotemporal shaping of multi-wavelength photon pulses

The experimental setup is depicted in Fig. 2, which mainly includes a 4-user fully-connected network based on quantum entanglement and the Fourier-transform apparatus. The second harmonic of an 5-picosecond pulsed laser is used to generate entangled photon pairs through the spontaneous parametric down conversion (SPDC) process in a periodically poled lithium niobate (PPLN) waveguide. By making use of telecommunications wavelength multiplexing and demultiplexing technology, we construct an entanglement-based quantum communication network with a fully connected architecture[5], which includes four users identified as Alice, Bob, Chole, and Dave, respectively (see Supplementary Note 1). Ultimately, six pairs of entangled photons are distributed among the four users and each user receives three wavelength-multiplexed channels simultaneously, ensuring they

can communicate with each other. One link of photon pulses is firstly sent to the spatiotemporal shaping apparatus to undergo the adaptive temporal and wavefront shaping, and then directed towards Alice via a 200-m-long MMF. The remaining quantum links are distributed to the other three users via single mode fibers directly. In our experiment, the lowest order mode (LP01) of the MMF whose intensity distribution is similar to that of a Gaussian beam is targeted to obtain the corresponding transmission matrix of the MMF by adaptive shaping. After transmission through the MMF, the reshaped photons are coupled into a single-mode fiber and detected by a superconducting nanowire single-photon detector (SNSPD) with a quantum efficiency of about 80%. All the detection events are recorded by a time-correlated single-photon counting (TCSPC), which provides feedback for the computer controlling the SLM to perform the spatiotemporal shaping.

In the Fourier-transform setup, a SLM leveraged to tailor the temporal profile and spatial wavefront of single photons. It has a resolution of 1920×1280 macropixels, each with a rectangular area of 8×8 μm. Given that each quantum link consists of three wavelength-multiplexed channels of entangled photons, the SLM is first divided into three rectangular components according to the position of different photon pulses spectrally dispersed by the grating, each comprising 640×1280 independently controllable macropixels with a varying phase $\theta \in [0, 2\pi]$. Aiming at the improvement of the distribution process of single photons, the phase of each macropixel starts with a set of random phase patterns and is iteratively optimized by the genetic algorithm based on a merit function, which is set as: $\mathcal{R}_t = \mathcal{C}_{opt}/\mathcal{C}_{ref}$, where $\mathcal{C}_{opt}$ and $\mathcal{C}_{ref}$ represent the detected photon count for the optimized-phase and flat-phase on the SLM, respectively. The detection result of the single photons provided by the SNSPD and TCSPC serves as a feedback signal for the genetic algorithm controlling the SLM. It is worth noting that the entanglement distribution process for all the multiplexed photon channels can be optimized simultaneously since they can be distinguished by using the time tag function.

Figure 2 shows the experimental results for the proposed spatiotemporal scheme. The optimization process in Fig. 2a presents the maximal values at each iteration of the genetic algorithm for all photon channels distributed to Alice. There is an obviously growing tendency for all the channels that have more photons coupled into the single mode fiber to be detected by the SNSPD, meaning that part of photons with a high-order mode has been transferred to the lowest order mode of the MMF. Figure 2b shows significant enhancement for the optimized SLM pattern shown in the inset, compared with a flat phase at optimal mechanical focus alignment, a reference case in which the SLM serves as a mirror and the manual coupling maximizes the peak. The growth factors after 300 iterations for CH35, CH43 and CH52 are over 3, 6, and 15, respectively, which convincingly imply the frequency-insensitive characteristic of the spatiotemporal shaping scheme based on the Fourier-transform apparatus. The differences in the enhancement ratio for different frequency channels are mainly caused by the difference in the initial output speckle patterns owing to the frequency-sensitive mode coupling characteristics of the MMF. It should be emphasized that before the optimization procedure the system coupling from the MMF to SMF has been artificially adjusted to be the best, ensuring the improvement of entanglement distribution through the MMF is attributed to the genetic algorithm.

For comparison, we optimize the entanglement distribution process through the MMF by using the traditional wavefront shaping scheme shown in Fig. 1a. During this comparative experiment, all other experimental parameters, such as the initial output mode of the MMF, the number of input single photons and system detection efficiency, are kept the same as the optimization procedure for the frequency-insensitive spatiotemporal shaping scheme. The merit function of the genetic algorithm is set as the increase of the total count ratio $\mathcal{R}_{total}$ for all photon channels, i.e., CH35, CH43, and CH52. The typical experimental results are shown in Fig. 3. As one can see from the results, although the total count ratio $\mathcal{R}_{total}$ grows steadily in the optimum iterative procedure, the evolution curves for each single photon channel show an out of sync serrated shape, which severely limits the overall improvement of the entanglement distribution process through the MMF. In this scheme, the wavelength channel will have a good performance during the shaping process if its photon count ratio is set as the merit function of the genetic algorithm. However, the other channels may not perform well after the transmission through a frequency-sensitive scattering medium. Unlike the traditional scheme, the spatiotemporal shaping scheme based on the Fourier-transform apparatus has the ability of optimizing the entanglement distribution process through a complex medium for multi-wavelength channels simultaneously. Thus, our proposed spatiotemporal shaping scheme is more suitable for a multi-user quantum network to improve the entanglement distribution process through a frequency-sensitive environment.

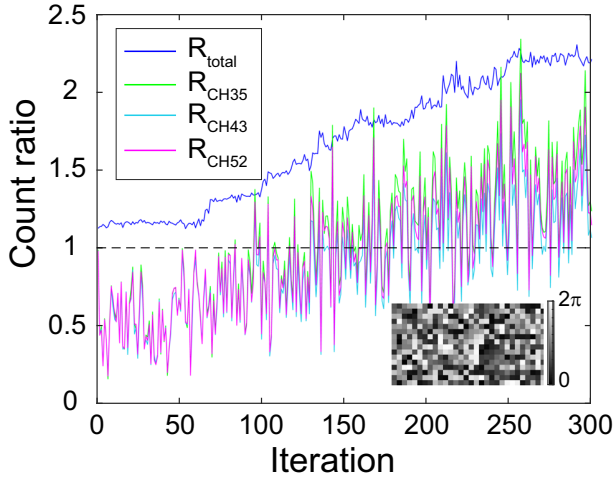

Fig. 3 Performance of the genetic algorithm for the traditional shaping setup. The inset presents the optimal phase pattern after the shaping process.

Quantum entanglement before and after spatiotemporal shaping

Maintaining quantum entanglement after spatiotemporal shaping is an important feature for a quantum spatiotemporal converter. Obviously, our Fourier-transform apparatus can serve as a coherent interface in a quantum network encoded in time-bin and time-energy DOF, to improve the entanglement distribution through a complex channel. To verify this feature, we measure the time-energy entanglement as an example, which is an inherent feature of photon pairs generated via cw laser-pumped SPDC. After the adaptive shaping process, we replace the pulse pump of the SPDC source with a cw laser and measure the time-energy entanglement by using a Franson-type interferometer[26], which consists of two 1-GHZ unbalanced Mach-Zehnder interferometers (MZI). The MZIs are made of free-space optical components and the relative phase between the two arms can be changed by applying the voltages to a resistive heater fixed on an optical element in the MZIs. We measure the Franson-type interference fringes of all the involved photon channels under two nonorthogonal phase bases before and after the spatiotemporal shaping. A flat phase mask and an optimized phase mask are applied to the spatial light modulator for the measurements before and after the spatiotemporal shaping,

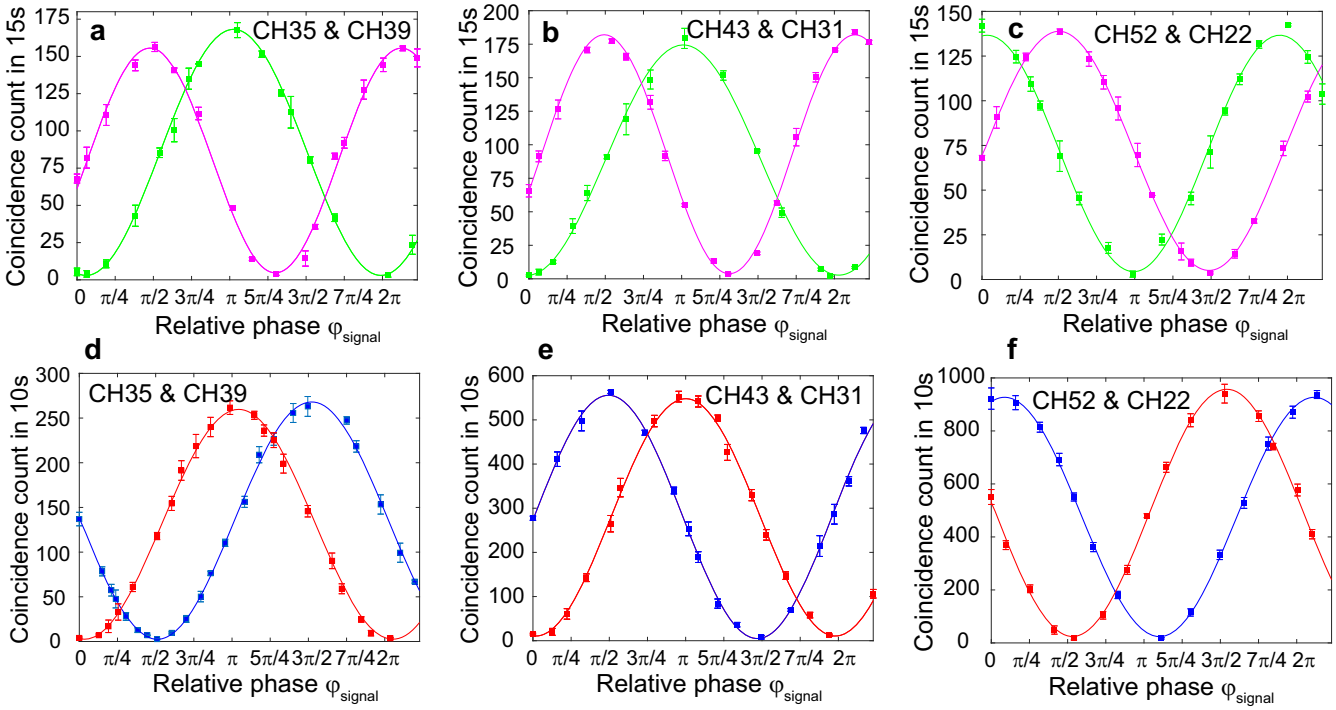

Fig. 4 Franson-type interference fringes before and after the spatiotemporal shaping. a–c Franson-type interference fringes before the spatiotemporal shaping. **d–f** Franson-type interference fringes after the spatiotemporal shaping. The error bars represent one standard deviation.

respectively. The experimental results are shown in Fig. 4, in which a-c and d-f are the interference fringes before and after the adaptively spatiotemporal shaping, respectively. We obtain the average fringe visibilities for the photon pairs CH35 & CH39, CH43 & CH31 and CH52 & CH22 after the spatiotemporal shaping to be $V = (N_{max} - N_{min})/(N_{max} + N_{min}) = 98.5\% \pm 0.5\%$, $97.4\% \pm 1.3\%$ and $96.8\% \pm 0.3\%$, respectively, while the average fringe visibilities before the spatiotemporal shaping are measured to be $96.5\% \pm 0.7\%$, $95.3\% \pm 1.8\%$ and $93.5\% \pm 0.7\%$. Such visibilities exceed the nonlocal bound of 71% of the Bell inequality and reveal a high quality of time-energy entanglement, which proves quantum entanglement can be well conserved during the spatiotemporal shaping. Therefore, our Fourier transform shaping setup can be used in a multi-user quantum network to improve the entanglement distribution through a frequency-sensitive complex scattering channel.

Optimal control of SFG process

To unequivocally demonstrate the versatility of the Fourier-transform apparatus, we further investigate the frequency-independent spatiotemporal shaping scheme by adaptively manipulating the SFG of single photons. After transmission through the MMF, the photons are upconverted to 780 nm in a PPLN waveguide pumped by three pulse lasers with a temporal pulse width of about 5 ps. See Supplementary Note 2 for the details of the experimental setup. To achieve the highest efficiency of SFG, one needs to produce additional quadratic temporal phases to the single photons to compensate for the second-order spectral dispersion[27,28] generated during transmission through the MMF, which is achieved by the spatiotemporal shaping scheme in our case. Figure 5a shows the efficiency of the SFG processes in the PPLN waveguide for Alice's photon channels. During the optimization processes, the SFG efficiency is controlled to be about 60%. The merit function for the genetic algorithm is set to be the optimized count ratio $\mathcal{R}_t^{sfg} = \mathcal{C}_{opt}^{sfg}/\mathcal{C}_{ref}^{sfg}$, where $\mathcal{C}_{opt}^{sfg}$ and $\mathcal{C}_{ref}^{sfg}$ represent the detected SFG photon count for the optimized-phase and flat-phase on the SLM, respectively. The performance of spatiotemporally optimized controlling the SFG process of single photons is depicted in Fig. 5b. After 300 iterations of optimization processes, the genetic algorithm provides an optimized control of SFG processes with an enhancement of 350%, 190%, and 160% for the photon channels CH35, CH43 and CH52, respectively, which highlights the versatility of spatiotemporal optimization that can control quantum light traversing different complex scattering media.

To be feasible as a quantum interface in practical networks, the quantum characteristics of the single photons should be preserved after frequency upconversion. To investigate this feature, we focus on the second-order autocorrelation function $g^2(\tau)$ of the SFG photons, which is a key parameter to characterize the figure-of-merit of a quantum field. During the experiment, the Hanbury Brown-Twiss interferometer[29] is leveraged to measure the $g^2(\tau)$ of the upconverted photons. Figure 6a shows a typical result of $g^2(0)$ and the corresponding coincidence-to-accidental ratio (CAR) of the entangled photon pairs between Alice and other users after SFG. Such a low autocorrelation and high CAR point to the high quality of the heralded single photon state and verify the single-photon character of the upconverted photons. Maintaining the quantum entanglement of signal photons during frequency conversion is essential for quantum network. For this important feature of the frequency convertor, there are several researches which show that the entangled characteristics can be well preserved during frequency up-conversion process[30–32]. One can easily characterize the time-bin entanglement by measuring the Franson-type interference fringes after frequency upconversion. Different from the original multi-wavelength signal photons with a spectral bandwidth of 100 GHz determined by the DWDM filters, the upconverted photons have a central wavelength of 780 nm and a spectral bandwidth of 0.08 nm, as shown in Fig. 6b, due to the quasi-phase match condition of the PPLN waveguide. The single-wavelength characteristic of the upconverted photons

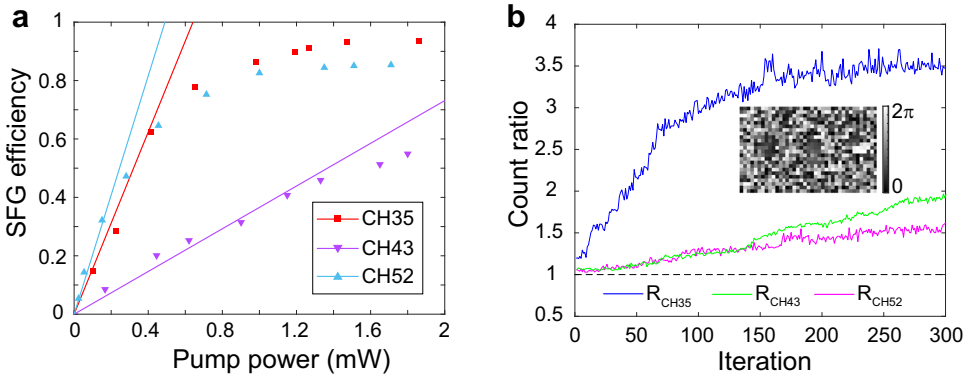

Fig. 5 Adaptive spatiotemporal shaping for enhancing the SFG process. a Experimental SFG efficiency versus pump power. **b** The genetic algorithm performance of spatiotemporal shaping. The inset presents the optimal phase pattern after the shaping process.

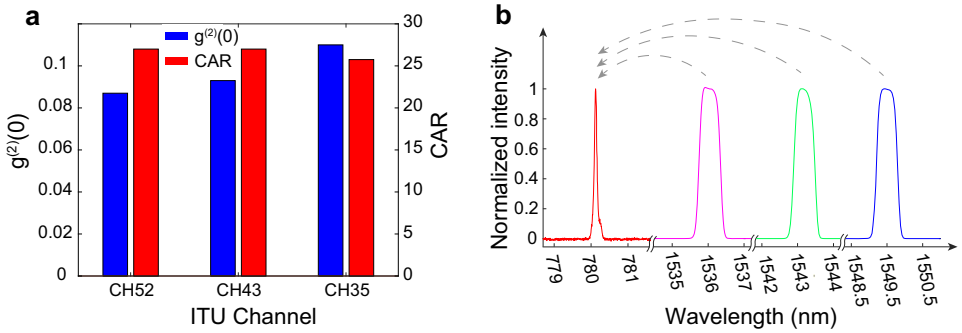

Fig. 6 Quantum characteristics and spectrum of the SFG photons. a The measured $g^2(0)$ and CAR after the SFG process. **b** Spectrum of single photons before and after the SFG process.

facilitates the following quantum information process in the network, such as quantum memory, entanglement swapping and teleportation which require to perform a HOM interference[33].

The future quantum network would be composed of heterogeneous quantum nodes based on entanglement encoded in different DOFs[34]. Obviously, our Fourier-transform apparatus can serve as a coherent interface in a large-scale quantum network encoded in time-bin and time-energy DOFs, to improve the entanglement distribution through a complex channel and help to establish a connection between remote nodes. Besides, the spatiotemporal wavefront shaping scheme can be easily extended to spatial entanglement[35] through a complex medium by performing appropriate projective measurements for the entangled state Fig. 6.

DISCUSSION

We implement the frequency-insensitive spatiotemporal shaping to control entangled photon pulses in a fully connected network propagating through a complex media. Based on a Fourier transform setup, our scheme can significantly improve the entanglement distribution process of multi-wavelength single photon pulses by adaptively compensating for the spatial and temporal disorder induced from the MMF. The optimization processes achieve a growth factor of over 300% for both linear entanglement distribution process and SFG processes. The quantum characteristics of the single photons are experimentally verified to be well preserved by certifying the time-energy entanglement and measuring the second-order autocorrelation function after the spatiotemporal shaping. Therefore, our scheme can serve as a bridging technology to establish the entanglement between remote nodes of spectrally interconnect quantum systems, which is an essential prerequisite for constructing a practical long-distance large-scale quantum network.

DATA AVAILABILITY

The data and code that support the plots within this paper and other findings of this study are available from the corresponding author upon reasonable request.

Received: 28 March 2023; Accepted: 21 August 2023;
Published online: 02 September 2023

REFERENCES

1. Wehner, S., Elkouss, D. & Hanson, R. Quantum internet: A vision for the road ahead. *Science* **362**, eaam9288 (2018).
2. Degen, C. L., Reinhard, F. & Cappellaro, P. Quantum sensing. *Rev. Mod. Phys.* **89**, 035002 (2017).
3. Guo, X. et al. Distributed quantum sensing in a continuous-variable entangled network. *Nat. Phys.* **16**, 281–284 (2020).
4. Chen, Y. A. et al. An integrated space-to-ground quantum communication network over 4,600 kilometres. *Nature* **589**, 214–219 (2021).
5. Wengerowsky, S., Joshi, S. K., Steinlechner, F., Hübel, H. & Ursin, R. An entanglement-based wavelength-multiplexed quantum communication network. *Nature* **564**, 225–228 (2018).
6. Joshi, S. K. et al. A trusted node–free eight-user metropolitan quantum communication network. *Sci. Adv.* **6**, eaba0959 (2020).
7. Xu, F., Ma, X., Zhang, Q., Lo, H. K. & Pan, J. W. Secure quantum key distribution with realistic devices. *Rev. Mod. Phys.* **92**, 025002 (2020).
8. Defienne, H., Reichert, M. & Fleischer, J. W. Adaptive quantum optics with spatially entangled photon pairs. *Phys. Rev. Lett.* **121**, 233601 (2018).
9. Lib, O. & Bromberg, Y. Quantum light in complex media and its applications. *Nat. Phys.* **18**, 986–993 (2022).
10. Cao, H., Mosk, A. P. & Rotter, S. Shaping the propagation of light in complex media. *Nat. Phys.* **18**, 994–1007 (2022).

11. Lib, O., Hasson, G. & Bromberg, Y. Real-time shaping of entangled photons by classical control and feedback. *Sci. Adv.* **6**, eabb6298 (2020).
12. Defienne, H., Barbieri, M., Walmsley, I. A., Smith, B. J. & Gigan, S. Two-photon quantum walk in a multimode fiber. *Sci. Adv.* **2**, e1501054 (2016).
13. Leedumrongwatthanakun, S. et al. Programmable linear quantum networks with a multimode fibre. *Nat. Photon.* **14**, 139–142 (2020).
14. Valencia, N. H., Goel, S., McCutcheon, W., Defienne, H. & Malik, M. Unscrambling entanglement through a complex medium. *Nat. Phys.* **16**, 1112–1116 (2020).
15. Amitonova, L. V., Tentrup, T. B., Vellekoop, I. M. & Pinkse, P. W. Quantum key establishment via a multimode fiber. *Opt. Express* **28**, 5965–5981 (2020).
16. Fisher, K. A. et al. Frequency and bandwidth conversion of single photons in a room-temperature diamond quantum memory. *Nat. Commun.* **7**, 1–6 (2016).
17. Ikuta, R. et al. Polarization insensitive frequency conversion for an atom-photon entanglement distribution via a telecom network. *Nat. Commun.* **9**, 1–8 (2018).
18. Weber, J. H. et al. Two-photon interference in the telecom c-band after frequency conversion of photons from remote quantum emitters. *Nat. Nanotechnol.* **14**, 23–26 (2019).
19. Lu, X. et al. Efficient telecom-to-visible spectral translation through ultralow power nonlinear nanophotonics. *Nat. Photon.* **13**, 593–601 (2019).
20. Tyumenev, R., Hammer, J., Joly, N. Y., Russell, P. S. J. & Novoa, D. Tunable and state-preserving frequency conversion of single photons in hydrogen. *Science* **376**, 621–624 (2022).
21. Ansari, V., Donohue, J. M., Brecht, B. & Silberhorn, C. Tailoring nonlinear processes for quantum optics with pulsed temporal-mode encodings. *Optica* **5**, 534–550 (2018).
22. Matsuda, N. Deterministic reshaping of single-photon spectra using cross-phase modulation. *Sci. Adv.* **2**, e1501223 (2016).
23. Mounaix, M. et al. Spatiotemporal coherent control of light through a multiple scattering medium with the multispectral transmission matrix. *Phys. Rev. Lett.* **116**, 253901 (2016).
24. Joshi, C. et al. Picosecond-resolution single-photon time lens for temporal mode quantum processing. *Optica* **9**, 364–373 (2022).
25. Monken, C. H., Ribeiro, P. S. & Pádua, S. Transfer of angular spectrum and image formation in spontaneous parametric down-conversion. *Phys. Rev. A* **57**, 3123 (1998).
26. Franson, J. D. Bell inequality for position and time. *Phys. Rev. Lett.* **62**, 2205 (1989).
27. Donohue, J. M., Agnew, M., Lavoie, J. & Resch, K. J. Coherent ultrafast measurement of time-bin encoded photons. *Phys. Rev. Lett.* **111**, 153602 (2013).
28. Karpiński, M., Jachura, M., Wright, L. J. & Smith, B. J. Bandwidth manipulation of quantum light by an electro-optic time lens. *Nat. Photon.* **11**, 53–57 (2017).
29. Brown, R. H. & Twiss, R. Q. Correlation between photons in two coherent beams of light. *Nature* **177**, 27–29 (1956).
30. Fisher, P., Cernansky, R., Haylock, B. & Lobino, M. Single photon frequency conversion for frequency multiplexed quantum networks in the telecom band. *Phys. Rev. Lett.* **127**, 023602 (2021).
31. VanDevender, A. P. & Kwiat, P. G. Quantum transduction via frequency upconversion. *JOSA B* **24**, 295–299 (2007).
32. Lenhard, A., Brito, J., Bock, M., Becher, C. & Eschner, J. Coherence and entanglement preservation of frequency-converted heralded single photons. *Opt. Express* **25**, 11187–11199 (2017).
33. Zhu, D. et al. Spectral control of nonclassical light pulses using an integrated thin-film lithium niobate modulator. *Light Sci. Appl.* **11**, 1–9 (2022).
34. Huang, Y. et al. A two-way photonic quantum entanglement transfer interface. *npj Quantum Inf.* **8**, 8 (2022).
35. Goel, S. et al. Inverse-design of high-dimensional quantum optical circuits in a complex medium. Preprint at https://arxiv.org/abs/2204.00578 (2022).

ACKNOWLEDGEMENTS

This work is supported in part by the National Natural Science Foundation of China (Grant Nos. 11734011, 11804135, and 12074155), The Foundation for Shanghai Municipal Science and Technology Major Project (Grant No. 2019SHZDZX01-ZX06), SJTU No. 21X010200828 and Jiangxi Provincial Natural Science Foundation (Grants No. 20212ACB201004, Grant No.20202ACBL211003).

AUTHOR CONTRIBUTIONS

X.C. led the project since its conception and supervised all experiments. Y.H., Z.Q. and Y.Y. performed the experiment and data analysis. Y.S., Y.T., F.Ni. and L.L. developed the feedback-control system based on genetic algorithm. All authors participated in discussions of the results. Y.H. prepared the manuscript with assistance from all other co-authors. Y.L., Y.Z. and X.C. provided revisions.

COMPETING INTERESTS

The authors declare no competing interests.

ADDITIONAL INFORMATION

Supplementary information The online version contains supplementary material available at https://doi.org/10.1038/s41534-023-00752-2.

Correspondence and requests for materials should be addressed to Xianfeng Chen.

Reprints and permission information is available at http://www.nature.com/reprints

Publisher's note Springer Nature remains neutral with regard to jurisdictional claims in published maps and institutional affiliations.